Nano Research

Open Access

Research Article

Edge detection and graph coloring by network of oscillatory neuromorphic devices comprising silicon nanosheet-gated diodes

Yunwoo Shin, Hyojoo Heo, Kyoungah Cho ✉, and Sangsig Kim ✉

Department of Electrical Engineering, Korea University, 145 Anam-ro, Seongbuk-gu, Seoul 02841, Republic of Korea

Cite this article: *Nano Research*, **2025**, *18*, 94907214. https://doi.org/10.26599/NR.2025.94907214

ABSTRACT: Oscillatory neural networks (ONNs) can handle image processing and combinational optimization problems with high biological plausibility. Coupled oscillators in ONNs mimic the neuronal oscillations and communication in the human brain. In this study, we demonstrate edge detection and graph coloring using a network of oscillatory neuromorphic devices comprising silicon nanosheet (NS)-gated diodes and series resistors. Silicon NS-gated diodes modulate the energy band structure in the channel through electrostatic doping, which tunes the amplitude and frequency of the oscillatory neuromorphic devices. Coupled oscillatory neuromorphic devices with capacitors can be in- or out-of-phase, enabling edge detection. Horizontal and vertical edge detections were performed using the coupling configuration. Furthermore, an ONN using oscillatory neuromorphic devices with resistive and capacitive couplings can solve graph coloring problems by representing the coloring solutions as phase differences. This study provides a method for achieving a compact silicon-based ONN that acts as a solver machine, as well as an image processor.

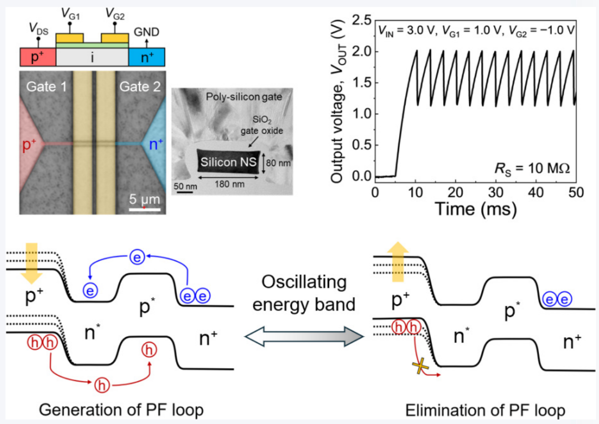

KEYWORDS: oscillatory neural network, silicon nanosheet-gated diode, positive feedback loop mechanism, edge detection, graph coloring

1 Introduction

Oscillatory neural networks (ONNs), inspired by nature, have attracted considerable attention as power-efficient neuromorphic computing architectures. Coupled oscillators in an ONN can mimic neuronal oscillations (e.g., brain waves) and communication in the human brain for processing and learning [1–4]. In an ONN, rich data mapping with high energy efficiency can be achieved by carrying information in the phase and frequency domains [5–8]. Recently, researchers have demonstrated the wide applicability of ONNs in image recognition and vowel classification through the phase synchronization of coupled oscillators [9–11]. Furthermore, ONNs have been extensively researched to solve combinational optimization problems (COPs) such as graph coloring and MAX-cut; the coupling strengths between oscillators in ONNs determine their phases to minimize the total energy of a system, which is known as the Kuramoto model [8, 12–15].

Compact oscillators have emerged as novel alternatives to oscillators comprising complementary metal-oxide-semiconductor (CMOS) circuits, which have disadvantages such as a large footprint area and high power consumption [9, 12–22]. Compact oscillators have been proposed using various emerging devices, including VO_X or NbO_X-based metal-insulator transition (MIT) devices and filamentary resistive switching devices [12–15, 18–22]. However, these oscillators encounter fundamental variation issues originating from their operating mechanisms. The electrical characteristics of MIT devices are highly temperature dependent (i.e., Joule heating), and the negative differential resistance and oscillating characteristics vanish at high temperatures [23, 24]. Resistive switching devices have considerable variations in switching voltages and high/low resistances because of filament formation and elimination mechanisms [25]. Although compact oscillators exhibit improved efficiency and CMOS compatibility, reliability issues remain, which cause fabrication nonuniformity [12, 20, 22].

Hence, we propose new oscillatory neuromorphic devices comprising series resistors and silicon nanosheet (NS)-gated diodes

Received: September 23, 2024; **Revised:** December 7, 2024
Accepted: December 25, 2024

✉Address correspondence to Kyoungah Cho, chochem@korea.ac.kr; Sangsig Kim, sangsig@korea.ac.kr

that have reliable electrical characteristics and high fabrication uniformity owing to mature CMOS technology. The gated diodes exhibit steep switching and bistable characteristics owing to their positive feedback (PF) loop and energy band modulation [26]. Unlike other oscillators, our oscillatory neuromorphic devices can tune the oscillation amplitudes and frequencies owing to the modulation of the energy band and carrier injection of the gated diodes. Furthermore, coupled oscillatory neuromorphic devices in ONNs are suitable as image-edge detectors and graph-coloring problem-solvers.

2 Results and discussion

Figure 1(a) shows the schematic and microscopic images of a silicon NS-gated diode on a silicon-on-insulator (SOI) wafer (180 nm × 80 nm). The gated diode is composed of heavily p-doped (p^+) drain, n-doped (n^+) source, and intrinsic (i)-channel regions. As shown by transmission electron microscopy (TEM), the SiO_2 gate oxide and two poly-silicon gates (2.0-μm wide) surround the i-channel region; thus, the omega-shaped gate stack enhances electrostatic doping. Gates 1 and 2 voltages (V_{G1} and V_{G2}, respectively) induce electrostatically n-doped (n^*) and p-doped (p^*) regions in the i-channel region via electrostatic doping, respectively, modulating the energy band structure of the p^+–n^*–p^*–n^+ layer.

The band structure is crucial for the PF-loop mechanism and tunable oscillations. The drain-source voltage (V_{DS}) injects holes into the i-channel region from the p^+ drain region. The gated diode exhibited steep switching and bistable characteristics owing to the PF loop mechanism, as shown in Fig. 1(b). With the forward sweep of V_{DS}, the hole injection increases so that the PF loop is generated at a V_{DS} of 1.82 V (called latch-up voltage, $V_{latch\text{-}up}$), showing that the drain-source current (I_{DS}) abruptly increases with a subthreshold swing of below 1 mV/dec. In contrast, the hole injection decreases during the reverse sweep of V_{DS}; therefore, I_{DS} abruptly decreases with the elimination of the PF loop at a latch-down voltage ($V_{latch\text{-}down}$) of 1.04 V. Figure 1(c) shows the oscillation operation of an oscillatory neuromorphic device with an input voltage (V_{IN}) of 3.0 V, a V_{G1} of 1.0 V, and a V_{G2} of −1.0 V. The device comprises a gated diode and a series resistor (R_S = 10 MΩ) connected to the p^+ drain electrode. The operating mechanism of the oscillatory neuromorphic device is illustrated in Fig. 1(d) with the corresponding energy band structures of a gated diode. As the output voltage (V_{OUT}) increases to 2.0 V, the energy level of the p^+ drain region decreases and hole injection increases, which is similar to the forward sweep of V_{DS}. When V_{OUT} reaches 2.0 V to generate the PF loop, the gated diode is turned on with a response time of 26 ns, and charge carriers flow through the diode (see Fig. S1 in the Electronic Supplementary Material (ESM)). Subsequently, V_{OUT} and hole injection from the p^+ drain region abruptly decreased until the PF loop was eliminated, which is similar to the reverse sweep of V_{DS}. Therefore, the oscillation characteristics stem from the oscillating energy band of the gated diode, and the PF loop mechanism of the silicon NS-gated diode guarantees reliability [27]. Furthermore, the silicon NS structure of the gated diode is critical to the oscillation characteristics stemming from the sequential switching operations of the gated diode (i.e., turn-off from the ON to OFF states and turn-on from the OFF to ON states). The NS structure contributes to rapid accumulation (recombination) of charge carriers by enhancing the gate controllability and reducing the demand of charge carriers for generation (elimination) of the PF loop. Hence, the NS-gated diodes are turned on and off more rapidly, enabling their oscillation behaviors with the fast-switching characteristics.

The tunable characteristics of an oscillatory neuromorphic device comprising a silicon NS-gated diode were achieved via energy-band modulation. V_{G1} modulates the energy level of the n^* region of the gated diode through electrostatic doping; herein, the potential barrier for hole injection from the p^+ drain region is built into the n^* region (Fig. 2(a)). $V_{latch\text{-}up}$ is positively shifted with the increase in V_{G1} in the I_{DS}–V_{DS} curves, as shown in Fig. 2(b). As the potential barrier for hole injection increases, a PF loop is generated at a larger V_{DS}. The oscillation frequency (f_{osc}) is expressed by Eq. (1), in which the oscillation amplitude is directly related to the $V_{latch\text{-}up}$ and $V_{latch\text{-}down}$ [28]

$$f_{osc} = \frac{V_{IN}}{R_S} \times \frac{1}{\text{Oscillation amplitude} \times C_{total}} \quad (1)$$

where C_{total} includes the intrinsic and parasitic capacitances of the

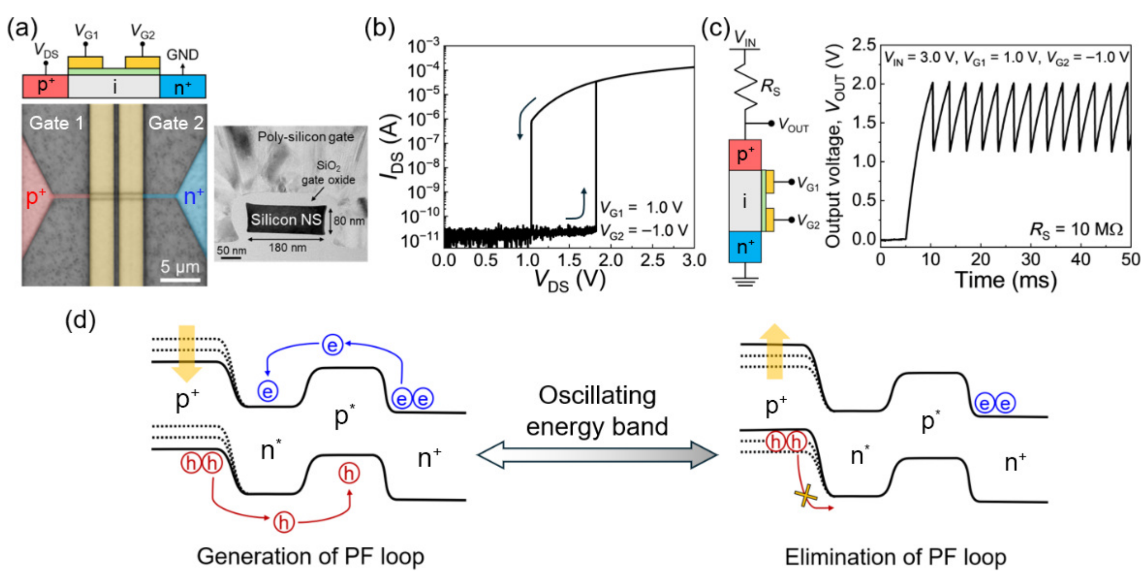

Figure 1 Oscillatory neuromorphic devices comprising silicon NS-gated diode. (a) Schematic and microscopic images and (b) switching curve of gated diode. (c) Oscillating operation and (d) mechanism of oscillator comprising gated diode and series resistor (R_S = 10 MΩ) with energy band structure.

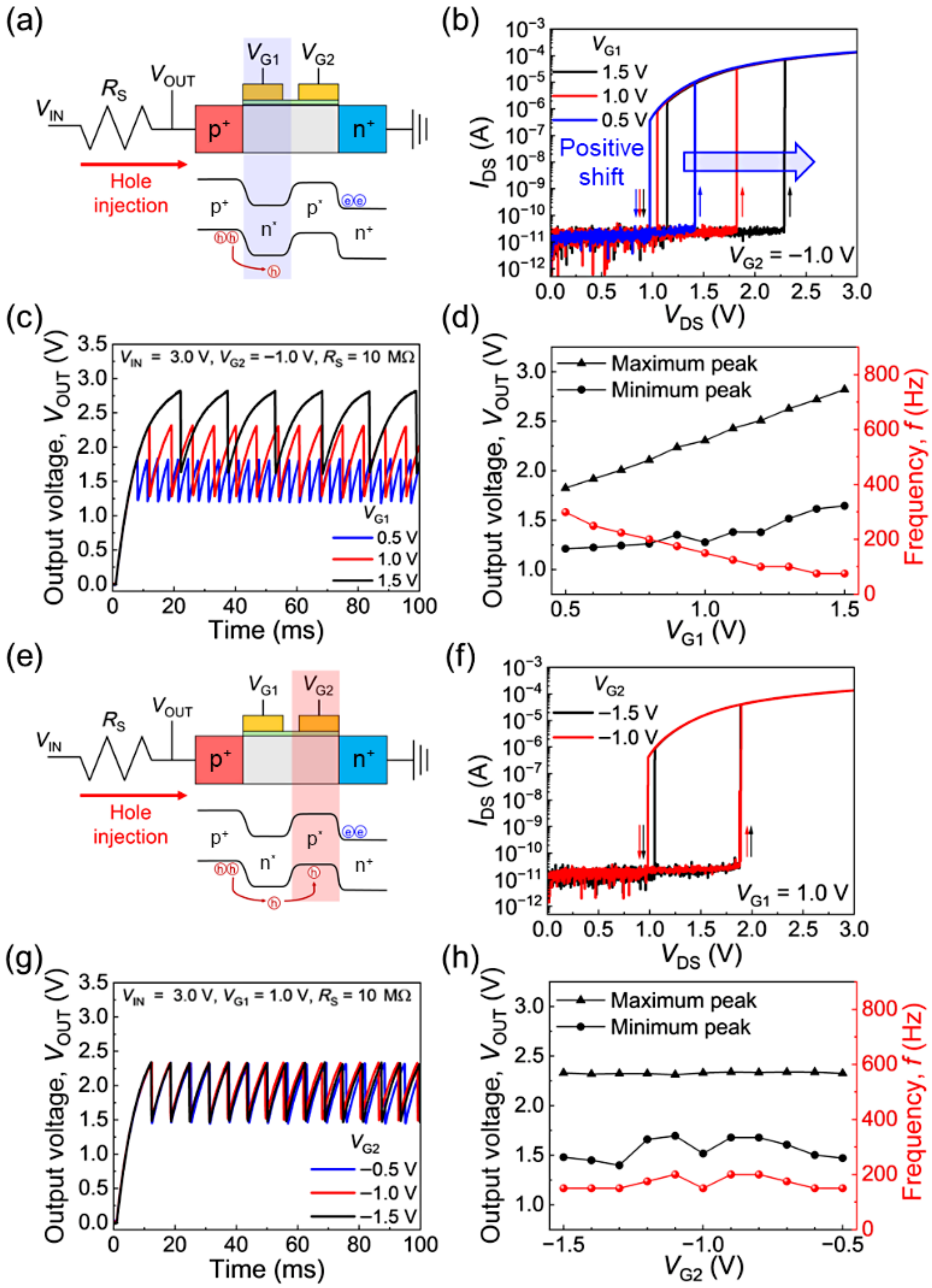

Figure 2 Tunable characteristics of oscillatory neuromorphic device. Schematics, switching curves, and tunable oscillating characteristics by variations in (a)–(d) V_{G1} and (e)–(h) V_{G2}.

silicon NS-gated diode and the measurement equipment. The capacitance of the gated diode comprises the barrier and diffusion capacitances in the OFF and ON states, respectively. The capacitance components were analyzed in detail using a technology computer-aided design simulation (Sentaurus, ver. T-2022.03-SP1) (see Fig. S2 in the ESM). f_{osc} was also proportional and reciprocal to V_{IN} and R_S, respectively (see Fig. S3 in the ESM). $V_{latch\text{-}up}$ and $V_{latch\text{-}down}$ are adjusted by modulating the potential barrier height for hole injection; thus, the oscillation properties are tunable by varying V_{G1}, as shown in Figs. 2(c) and 2(d). However, the switching and oscillation properties are irrelevant to V_{G2}; V_{G2} modulates the depth of the potential well in the p* region, where the injected holes accumulate (Figs. 2(e)–2(h)). The generation and elimination of the PF loop were mainly affected by carrier injection rather than by carrier accumulation. Moreover, the silicon-gated diode can utilize electrons as the major charge carriers for the PF loop mechanism (see Figs. S4 and S5 in the ESM). Unlike previously reported oscillators, the proposed oscillatory neuromorphic device can tune the oscillation properties by electrostatic doping owing to the PF loop mechanism of the diode. Consequently, the tunable oscillatory neuromorphic device is a promising candidate for the construction of a reliable ONN because it is free from fabrication non-uniformity.

To investigate the feasibility of the ONN using oscillatory neuromorphic devices as edge detection filters, we coupled two devices with a coupling capacitor (C_C = 10 pF), as shown in Fig. 3(a). The time delay (ΔT_{IN}) of two input voltages (V_{IN1} and V_{IN2}) of the coupled oscillatory devices corresponds to the difference between two adjacent pixel values in an input image. Figure 3(b) shows the in- and out-of-phase states. If the values of two pixels are the same (i.e., ΔT_{IN} = 0.0 ms), the phases of the oscillatory devices are the same (i.e., in-phase synchronization). Thus, the two pixels were not at the edge of the image, and the pixels were processed as black. In the other cases (ΔT_{IN} = 0.5 and 1.0 ms), the oscillatory devices settle to out-of-phase in which the two pixels are in an edge part of the image so that the pixels are processed as white. The coupled oscillatory devices can perform edge detection by processing the pixels of an input image in the time domain (i.e., ΔT_{IN}) and settling to in- or out-of-phase according to the ΔT_{IN} [12]. Figure 3(c) shows the results of the edge-detection simulation, in which the oscillatory devices coupled in the vertical (horizontal) direction detect the horizontal (vertical) edges of the image. Thus, edge detection depends on the configuration of the filters, even though they process the same part (window) of the input image. In this study, the oscillatory neuromorphic devices comprise the silicon NS-gated diodes with capacitive coupling function as an edge detection filter in the image processing. As a first step of the image processing, the filter takes the image pixels as input voltages of oscillators and detects the edge parts of the image by leveraging the phase differences of the coupled oscillators. Thereafter, the image processing such as anti-aliasing is performed selectively to the edge parts, which reduces the workload and improves the performance of graphic processing units [29, 30]. Consequently, the proposed ONN can be utilized as a hardware-based edge detection filter for high-performance image processors.

Furthermore, the ONN comprising the oscillators can solve the graph coloring problems that belong to the class of nondeterministic polynomial-hard combinatorial problems. Hence, the ONN can be used in applications including scheduling or register allocation in compliers as well as map coloring. In ONN, the coupling configurations of the oscillators determine the phase of the coupled oscillators to minimize the total energy of the system. The coupling strength depends on the coupling configuration. As shown in Figs. 4(a) and 4(b), the oscillators coupled with a capacitor (C_C) with 100 pF settle to out of phase. When the gated diode of the left-side oscillator was turned on, V_{OUT1} decreased abruptly as charge carriers flowed to the ground (GND). Then, the V_{OUT2} drops because charge carriers in the output node of the right oscillator leak to GND through the C_C, and *vice versa*. In contrast, the oscillators coupled with a resistor (R_C) with 100 kΩ show the in-phase synchronization as represented in Figs. 4(c) and 4(d); the output nodes share charge carriers by voltage division because the R_C is smaller than the R_S and off resistance of the gated diode. In short, R_C (C_C) represents a strong (weak) coupling between the oscillators because of voltage division (current leakage).

Figure 5(a) shows the coupling configuration in the ONN used to solve the graph-coloring problem, where each vertex (1–4) corresponds to an oscillatory neuromorphic device (DO1–DO4),

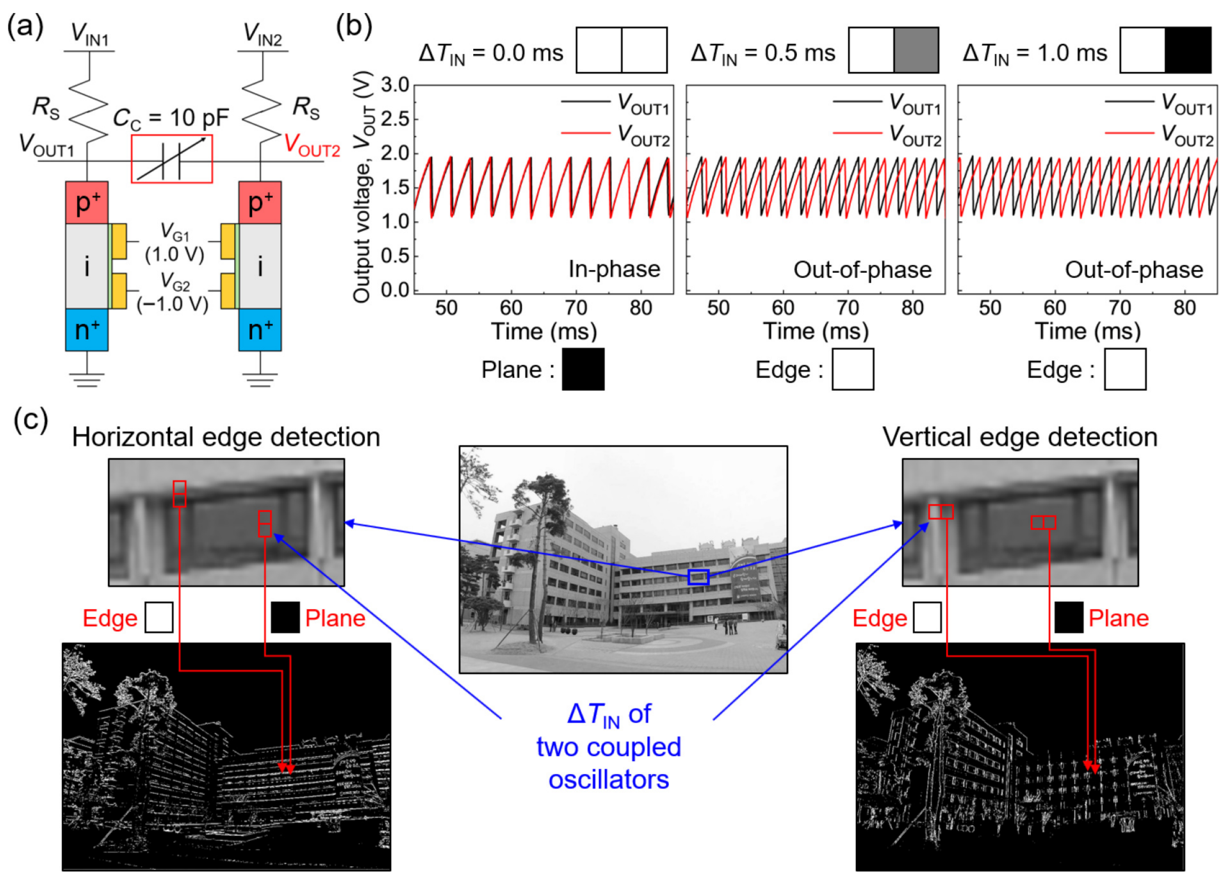

Figure 3 Edge detection of two coupled oscillatory neuromorphic devices. (a) Circuit diagram and (b) synchronization of two coupled oscillatory neuromorphic devices according to ΔT_{IN}. (c) Horizontal and vertical edge detection simulations.

Tsinghua University Press | SciOpen

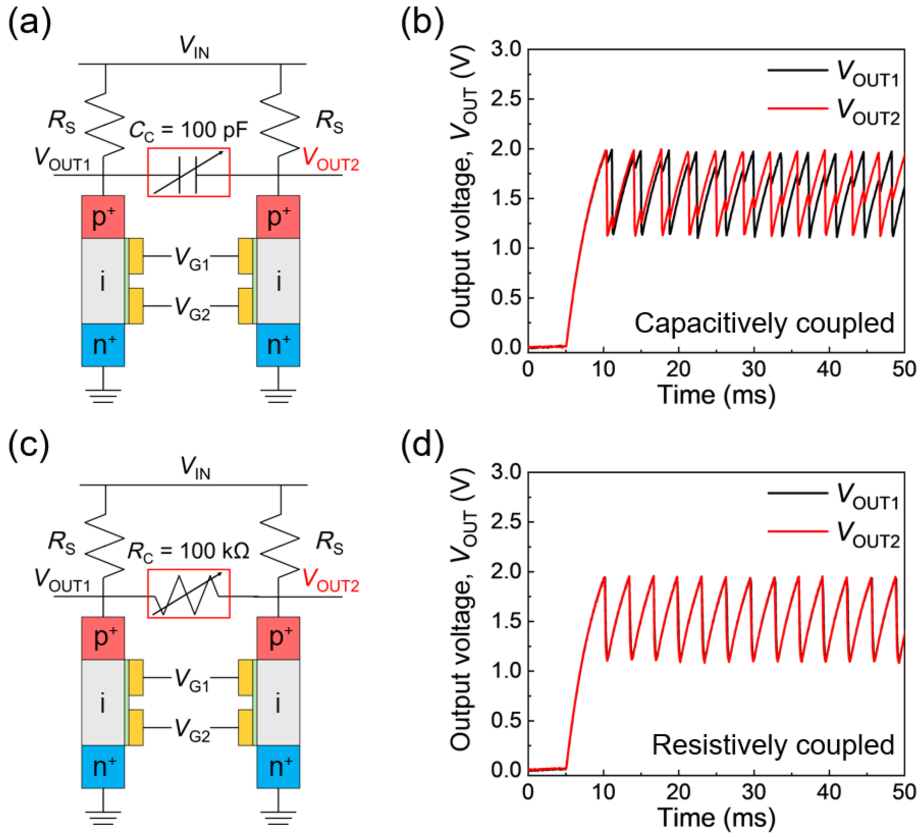

Figure 4 Coupling characteristics. Circuit diagrams and synchronizations of two coupled oscillatory neuromorphic devices with ((a) and (b)) a capacitor (C_C = 100 pF) and ((c) and (d)) a resistor (R_C = 100 kΩ).

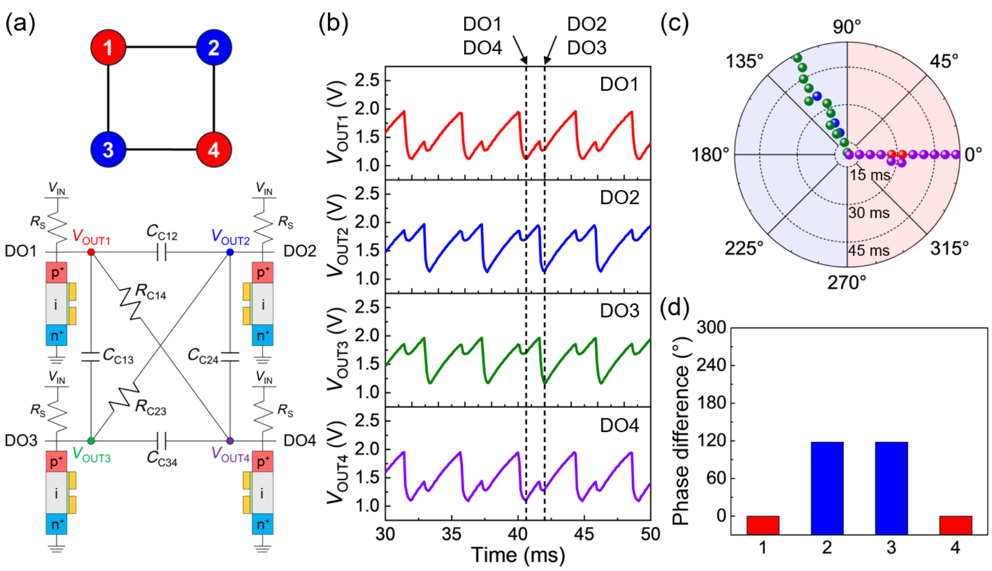

Figure 5 ONN using oscillatory neuromorphic devices comprising silicon NS-gated diodes for a graph coloring problem. (a) input graph and circuit diagram. (b) oscillating operations, (c) time-dependent phase plot, and (d) phase differences of four coupled oscillatory devices.

and the connections between the vertices are represented as the coupling strengths (i.e., R_C for strong coupling and C_C for weak coupling) between the oscillatory neuromorphic devices. We note here that in the graph coloring, there are no two adjacent vertices with the same color. A timing diagram of the output voltages of four coupled oscillatory devices is shown in Fig. 5(b), where the dashed lines represent the phases of four oscillatory devices. The line patterns reveal that DO1 and DO4 (DO2 and DO3) are stabilized in phase because they are strongly coupled with R_{C14} (R_{C23}). The phases of DO2 and DO3 differ from those of DO1 and DO4. The phase differences between four coupled oscillatory devices that vary with time are plotted in Fig. 5(c), using the phase of DO1 as a reference. The passage of time is expressed as the radius of the circle, whose center and circumference are 10 and 55 ms, respectively. The phases were stabilized in the two cases over time because four coupled oscillatory devices mutually interacted with each other. In this graph, the vertices are assigned different colors (red and blue) if the oscillatory devices have phase differences greater than ±90°. Figure 5(d) shows the phase differences of the oscillatory devices extracted at 50 ms. DO2 and DO3 have phase differences of approximately 120° compared to DO1 and DO4. The graph-coloring problem (i.e., vertices 1 and 4 for red and vertices 2 and 3 for blue) was successfully solved using the phase differences of the oscillatory devices that map the input graphs.

Various graph-coloring problems can be solved using ONN. Figure 6(a) illustrates various input graphs that can be mapped to ONNs in the same manner as that shown in Fig. 5(a). The time-dependent phases of the coupled oscillatory devices sustain the differences between them (Fig. 6(b)); herein, the time scale is the same as that shown in Fig. 5(c). In some cases, time is required to stabilize the phases because of the interactions between the coupled oscillatory devices corresponding to the input graphs. Regardless of the input graphs, the proposed oscillatory devices can simplify the ONN coloring algorithm, which assigns colors to vertices with phase differences. In this sense, the proposed ONN is superior to previous ONNs that require appropriate algorithms depending on the input graphs [15, 18]. For all cases in Fig. 6(c), the vertexes in the same color have phase differences within ±45°. Hence, the oscillatory devices can solve the graph coloring problems by taking the phase difference of ±45° as a standard. Consequently, the ONN using our oscillatory neuromorphic devices comprising the silicon NS-gated diodes demonstrated the feasibility of compact silicon-based solver machines.

Table 1 presents a comparison between our oscillatory neuromorphic device comprising the silicon NS-gated diode and other oscillators comprising various emerging devices [5, 16, 21, 23, 24]. The oscillation characteristics of the oscillators arise from the sequential state transitions of the comprising devices, and thereby the endurance and reliability of the devices are critical properties for implementing oscillators. In this regard, there is the advantage of the silicon NS-gated diode since the unique operating mechanism of the gated diode does not cause any degradation of the diode. In terms of the auxiliary circuit, which is closely related to the area

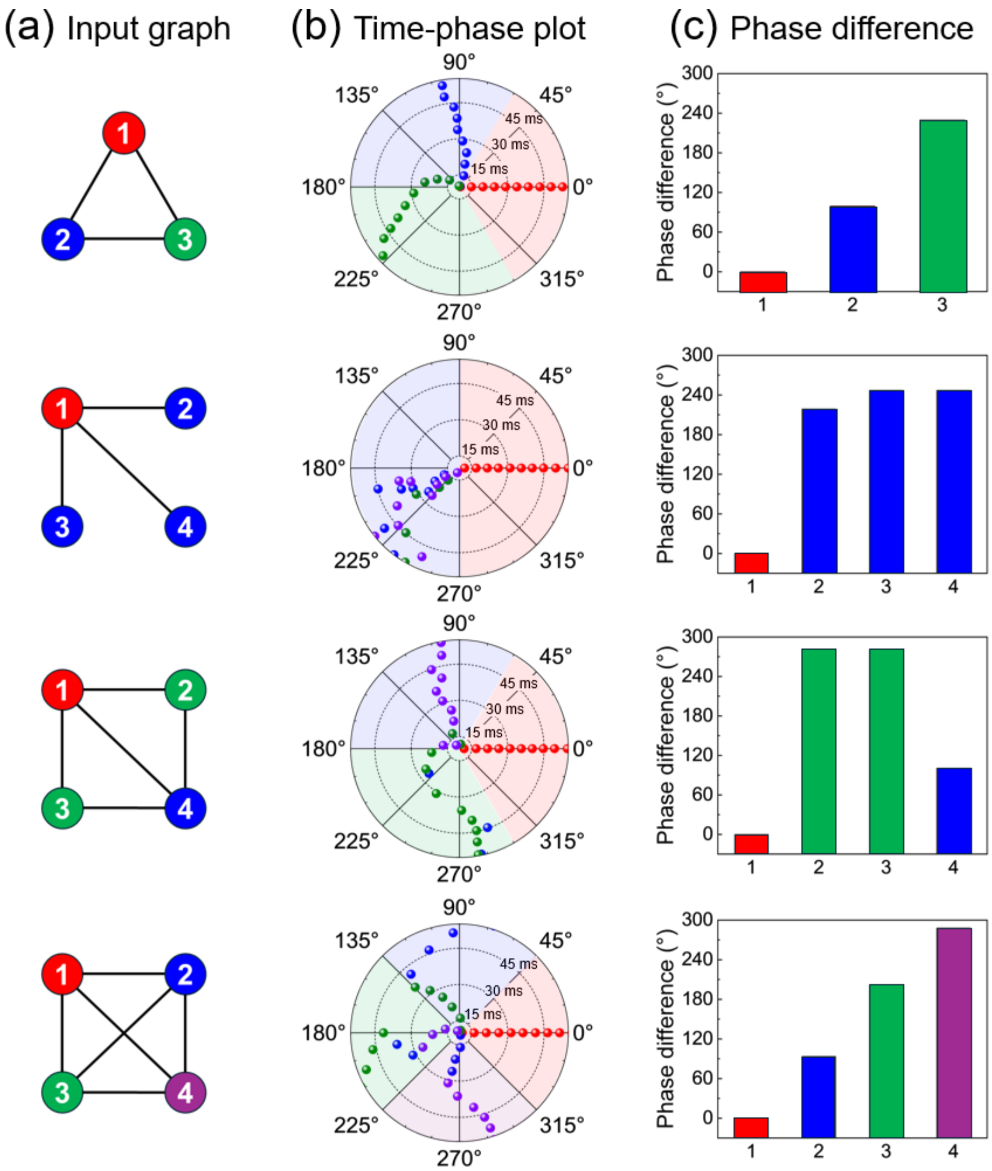

Figure 6 Various graph coloring problems. (a) Input graphs. (b) Time-dependent phase plots and (c) phase differences of our oscillatory neuromorphic devices coupled according to input graphs in the same manner as those in Fig. 5(a).

清华大学出版社 Tsinghua University Press | SciOpen

Table 1 Comparison between our oscillatory neuromorphic device and other oscillators

Devices, auxiliary circuit	Oscillation mechanism	Operating voltage (V)	Number of coupled oscillators (experimental)	Application
NbO_2 MIT device [5], 1R	Metal-insulator transition	4.0	2	Pattern recognition
VO_2 MIT device [16], 1R + 1C	Metal-insulator transition	5.0	9	Graph coloring, MAX-cut, MAX-3SAT[c]
Ag/h-BN[a] memristor [21], 1R + 1C	Resistive filament formation	0.28	4	Graph coloring, MAX-cut
TaO_X RRAM[b] [23], 1T	Resistive filament formation	7.0	2	—
SiO_X RRAM [24], 1R	Resistive filament formation	3.0	2	Pattern recognition
Silicon NS-gated diode (this work), 1R	Energy band modulation	3.0	4	Edge detection, graph coloring

[a]h-BN: hexagonal boron nitride. [b]RRAM: resistive random access memory. [c]3SAT: 3-satisfiability.

efficiency of the ONN, the proposed oscillatory device is similar to or superior to the others. The operating voltage and number of experimentally coupled oscillators were comparable or superior to those of the other methods. Furthermore, the ONN comprising our oscillatory neuromorphic devices demonstrate wide applicability to edge detection and graph coloring. Besides, the proposed oscillatory neuromorphic devices allow for tunable oscillation amplitude and frequency by modulating the gate voltages of the gated diodes, unlike other oscillators. Additionally, the ONN comprising the silicon NS-gated diodes holds promise for seamlessly implementing neuromorphic hardware because they are fully compatible with CMOS fabrication processes. Consequently, oscillatory neuromorphic devices constructed with the silicon NS-gated diodes can be used to realize compact silicon-based ONN for image processors and solver machines.

3 Conclusions

In this study, we designed a network of tunable oscillatory neuromorphic devices to perform edge detection and solve the coloring problems. The tunable oscillatory devices comprise silicon NS-gated diodes and series resistors, and energy-band modulation enables tunable oscillation characteristics. In the edge detection of capacitively coupled oscillatory neuromorphic devices, the configuration of the device determines whether the pixels of the input image in the time and phase domains are processed via horizontal or vertical edge detection. Furthermore, the coloring problems are solved using the phase differences of the resistively and capacitively coupled oscillatory devices that map the input graphs. Consequently, the proposed ONN consisting of oscillatory neuromorphic devices is a promising candidate for reliable neuromorphic computing, which enables image processing and COP solving.

4 Experimental

4.1 Device fabrication

The silicon NS-gated diodes were fabricated using full CMOS processes from a p-type (100)-oriented SOI wafer with a 100 nm thick top silicon active layer (doping concentration of 10^{16} cm^{-3}) and 2-μm thick buried oxide layer. First, a silicon NS layer with a width of 180 nm was formed via photolithography and dry etching. Then, two poly-silicon gate electrodes (thick = 400 nm and width = 2 μm) were formed with a 1-μm wide gap by low-pressure chemical vapor deposition (LPCVD) on a SiO_2 gate oxide layer, which was thermally grown on the intrinsic channel region at 850 °C. The p^+ drain and gate2 regions were heavily doped with difluoroboron ions at a dose of 3×10^{15} cm^{-2} and ion energy of 30 keV. The n^+ source and gate1 regions were heavily doped with P^+ ions at a dose of 3×10^{15} cm^{-2} and ion energy of 50 keV. Afterwards, the rapid thermal annealing process was carried out at 1050 °C for 30 s to activate the implanted dopants. Finally, a Ti/TiN/Al/TiN metal alloy was deposited in the drain, source, and gate contact regions after interlayer dielectric deposition using LPCVD-based tetraethyl orthosilicate, followed by an alloying process at 400 °C for 30 min. Subsequently, the wafer was first annealed at 1000 °C for 30 min in a nitrogen atmosphere, followed by rapid thermal annealing at 1050 °C for 30 s to activate the implanted dopants with uniform diffusion and eliminate defects. Finally, a Ti/TiN/Al/TiN metal alloy was deposited in the drain, source, and gate contact regions after the interlayer dielectric deposition using LPCVD-based tetraethylorthosilicate (TEOS).

4.2 Measurement

The switching characteristics of the silicon NS-gated diode were measured using a semiconductor parameter analyzer (HP4155C, Agilent). Keithley 2636A and 2636B source meters were used to measure the tunable and coupled characteristics of the oscillatory neuromorphic devices. The morphology of the fabricated diode was observed by optical microscopy (Nikon, Eclipse L150) and TEM (JEOL JEM-2100F, FEG).

Electronic Supplementary Material: Supplementary material (further analysis of the switching and oscillation characteristics) is available in the online version of this article at https://doi.org/10.26599/NR.2025.94907214.

Data availability

All data needed to support the conclusions in the paper are presented in the manuscript and the Electronic Supplementary Material. Additional data related to this paper may be requested from the corresponding author upon request.

Acknowledgements

This research was partly supported by a National Research Foundation of Korea (NRF) grant funded by the Korean government (Nos. 2022M3I7A3046571 and 2023RS00260876); the Brain Korea 21 Plus Project through the NRF funded by the Ministry of Science, ICT and Future Planning, Samsung Electronics (No. IO201223-08257-01); and a Korea University Grant.

Declaration of competing interest

All the contributing authors report no conflict of interests in this work.

Author contribution statement

Y. S. and H. H. provided conceptualization and methodology. Y. S. performed the edge detection simulation. Y. S., H. H., and K. C. verified and investigated. Y. S., K. C., and S. K. analyzed the results and wrote the manuscript. S. K. supervised the study. All authors edited and approved the final version of the manuscript.

Use of AI statement

None.

References

[1] Xu, M. Y.; Chen, X. R.; Guo, Y. H.; Wang, Y.; Qiu, D.; Du, X. C.; Cui, Y.; Wang, X. F.; Xiong, J. Reconfigurable neuromorphic computing: Materials, devices, and integration. *Adv. Mater.* **2023**, *35*, 2301063.

[2] Upadhyay, N. K.; Jiang, H.; Wang, Z. R.; Asapu, S.; Xia, Q. F.; Joshua Yang, J. Emerging memory devices for neuromorphic computing. *Adv. Mater. Technol.* **2019**, *4*, 1800589.

[3] Carapezzi, S.; Boschetto, G.; Delacour, C.; Corti, E.; Plews, A.; Nejim, A.; Karg, S.; Todri-Sanial, A. Advanced design methods from materials and devices to circuits for brain-inspired oscillatory neural networks for edge computing. *IEEE J. Emerg. Sel. Topics Circuits Syst.* **2021**, *11*, 586–596.

[4] Liu, H. F.; Qin, Y.; Chen, H. Y.; Wu, J. B.; Ma, J. H.; Du, Z. H.; Wang, N.; Zou, J. Y.; Lin, S.; Zhang, X. et al. Artificial neuronal devices based on emerging materials: Neuronal dynamics and applications. *Adv. Mater.* **2023**, *35*, 2205047.

[5] Kim, H. W.; Kang, S. Y.; Moon, J.; Kim, N.; Hong, E.; Jeon, S.; Jeon, S.; Woo, J. Experimental robust spontaneous synchronizations in coupled NbO_x oscillation neurons for unconventional computing. *IEEE Trans. Electron Devices* **2023**, *70*, 6699–6702.

[6] Kim, H. W.; Jeon, S.; Jeon, S.; Hong, E.; Kim, N.; Woo, J. Brain-inspired mutual synchronization in cross-coupled NbO_x oscillation neurons for oscillatory neural network applications. *IEEE Access* **2023**, *11*, 82443–82448.

[7] Csaba, G.; Porod, W. Coupled oscillators for computing: A review and perspective. *Appl. Phys. Rev.* **2020**, *7*, 011302.

[8] Kuramoto, Y. Self-entrainment of a population of coupled non-linear oscillators. In *International Symposium on Mathematical Problems in Theoretical Physics*. Araki, H., Ed.; Springer: Berlin, Heidelberg, 1975; pp 420–422.

[9] Nikonov, D. E.; Kurahashi, P.; Ayers, J. S.; Li, H.; Kamgaing, T.; Dogiamis, G. C.; Lee, H. J.; Fan, Y. P.; Young, I. A. Convolution inference via synchronization of a coupled CMOS oscillator array. *IEEE J. Explor. Solid-State Comput. Devices Circuits* **2020**, *6*, 170–176.

[10] Dutta, S.; Khanna, A.; Chakraborty, W.; Gomez, J.; Joshi, S.; Datta, S. Spoken vowel classification using synchronization of phase transition nano-oscillators. In *Proceedings of 2019 Symposium on VLSI Technology*, Kyoto, Japan, 2019, pp T128–T129.

[11] Romera, M.; Talatchian, P.; Tsunegi, S.; Abreu Araujo, F.; Cros, V.; Bortolotti, P.; Trastoy, J.; Yakushiji, K.; Fukushima, A.; Kubota, H. et al. Vowel recognition with four coupled spin-torque nano-oscillators. *Nature* **2018**, *563*, 230–234.

[12] Kim, H. W.; Jeon, S.; Kang, H.; Hong, E.; Kim, N.; Woo, J. Understanding rhythmic synchronization of oscillatory neural networks based on NbO_x artificial neurons for edge detection. *IEEE Trans. Electron Devices* **2023**, *70*, 3031–3036.

[13] Parihar, A.; Shukla, N.; Jerry, M.; Datta, S.; Raychowdhury, A. Vertex coloring of graphs via phase dynamics of coupled oscillatory networks. *Sci. Rep.* **2017**, *7*, 911.

[14] Maher, O.; Jiménez, M.; Delacour, C.; Harnack, N.; Núñez, J.; Avedillo, M. J.; Linares-Barranco, B.; Todri-Sanial, A.; Indiveri, G.; Karg, S. A CMOS-compatible oscillation-based VO_2 Ising machine solver. *Nat. Commun.* **2024**, *15*, 3334.

[15] Delacour, C.; Carapezzi, S.; Abernot, M.; Todri-Sanial, A. energy-performance assessment of oscillatory neural networks based on VO_2 devices for future edge AI computing. *IEEE Trans. Neural Netw. Learn. Syst.* **2024**, *35*, 10045–10058.

[16] Mallick, A.; Bashar, M. K.; Truesdell, D. S.; Calhoun, B. H.; Joshi, S.; Shukla, N. Graph coloring using coupled oscillator-based dynamical systems. In *Proceedings of 2021 IEEE International Symposium on Circuits and Systems* (*ISCAS*), Daegu, Korea, 2021, pp 1–5.

[17] Wu, C. W. Graph coloring via synchronization of coupled oscillators. *IEEE Trans. Circuits Syst. I: Fundam. Theory Appl.* **1998**, *45*, 974–978.

[18] Shubham, S.; Mohanty, S.; Lashkare, S. Fault tolerance of oscillatory neural network using PMO oscillator. In *Proceedings of 2024 8th IEEE Electron Devices Technology & Manufacturing Conference* (*EDTM*), Bangalore, India, 2024, pp 1–3.

[19] Chen, X.; Yang, D. L.; Hwang, G.; Dong, Y. J.; Cui, B. B.; Wang, D. C.; Chen, H. G.; Lin, N.; Zhang, W. Q.; Li, H. H. et al. Oscillatory neural network-based ising machine using 2D memristors. *ACS Nano* **2024**, *18*, 10758–10767.

[20] Delacour, C.; Carapezzi, S.; Abernot, M.; Boschetto, G.; Azemard, N.; Salles, J.; Gil, T.; Todri-Sanial, A. Oscillatory neural networks for edge AI computing. In *Proceedings of 2021 IEEE Computer Society Annual Symposium on VLSI* (*ISVLSI*), Tampa, USA, 2021, pp 326–331.

[21] Sharma, A. A.; Bain, J. A.; Weldon, J. A. Phase coupling and control of oxide-based oscillators for neuromorphic computing. *IEEE J. Explor. Solid-State Comput. Devices Circuits* **2015**, *1*, 58–66.

[22] Hong, E.; Kim, H. W.; Choi, H.; Jeon, S.; Kim, N.; Woo, J. Demonstration of threshold switching in undoped SiO_x layer for oscillation neurons. *IEEE Trans. Electron Devices* **2024**, *71*, 2228–2232.

[23] Das, S. K.; Nandi, S. K.; Marquez, C. V.; Rúa, A.; Uenuma, M.; Puyoo, E.; Nath, S. K.; Albertini, D.; Baboux, N.; Lu, T. et al. Physical origin of negative differential resistance in V_3O_5 and its application as a solid-state oscillator. *Adv. Mater.* **2023**, *35*, 2208477.

[24] Schofield, P.; Bradicich, A.; Gurrola, R. M.; Zhang, Y. W.; Brown, T. D.; Pharr, M.; Shamberger, P. J.; Banerjee, S. Harnessing the metal-insulator transition of VO_2 in neuromorphic computing. *Adv. Mater.* **2023**, *35*, 2205294.

[25] Li, Y. B.; Wang, Z. R.; Midya, R.; Xia, Q. F.; Yang, J. J. Review of memristor devices in neuromorphic computing: Materials sciences and device challenges. *J. Phys. D: Appl. Phys.* **2018**, *51*, 503002.

[26] Lim, D.; Cho, K.; Kim, S. Single silicon neuron device enabling neuronal oscillation and stochastic dynamics. *IEEE Electron Device Lett.* **2021**, *42*, 649–652.

[27] Lim, D.; Son, J.; Cho, K.; Kim, S. Quasi-nonvolatile silicon memory device. *Adv. Mater. Technol.* **2020**, *5*, 2000915.

[28] Han, J. K.; Seo, M.; Kim, W. K.; Kim, M. S.; Kim, S. Y.; Kim, M. S.; Yun, G. J.; Lee, G. B.; Yu, J. M.; Choi, Y. K. Mimicry of excitatory and inhibitory artificial neuron with leaky integrate-and-fire function by a single MOSFET. *IEEE Electron Device Lett.* **2020**, *41*, 208–211.

[29] Vijayarani, S.; Vinupriya, M. Performance analysis of canny and sobel edge detection algorithms in image mining. *Int. J. Innovative Res. Comput. Commun. Eng.* **2013**, *1*, 1760–1767.

[30] Kumar, S.; Upadhyay, A. K.; Dubey, P.; Varshney, S. Comparative analysis for edge detection techniques. In *Proceedings of 2021 International Conference on Computing, Communication, and Intelligent Systems* (*ICCCIS*), Greater Noida, India, 2021, pp 675–681.